

ELECTROTHERMAL BEHAVIOR AND MICROSTRUCTURAL CHARACTERISTICS OF ZINC OXIDE-BASED VARISTOR CERAMICS ¹

*José Geraldo de Melo Furtado*²
*Luiz Antônio Saléh*³
*Eduardo Torres Serra*⁴
*Jorge Henrique Greco Lima*⁵
*Maria Cecília de Souza Nóbrega*⁶

Abstract

The aspects concerned with the leakage current, energy absorption and heat dissipation capacity of a varistor under several operation conditions are very important to the design, the performance and the degradation behavior of these devices used in protection systems against overvoltages. The aim of this work is to evaluate the relationships between microstructural characteristics and the electrothermal stability of zinc oxide-based varistor ceramics. Scanning electron microscopy, X-ray energy dispersive spectroscopy, voltage-current characteristics, heat dissipation factor and densification level of the produced varistors were used to evaluate the relationships between ceramic processing parameters, microstructural aspects and the varistor properties of several zinc oxide-based ceramics produced. The results evidence that the leakage current, energy absorption and heat dissipation capacity of a varistor depend of various parameters, such as densification level, precipitated phases distribution, grain size distribution and compositional homogeneity, beyond the specific chemical composition of the device, specially the dopants nature. Rare-earth-zinc oxide-based varistors, exhibiting simpler microstructure, present better dielectric behavior. For a fixed chemical composition, a narrow size particle distribution resulted in smaller values of leakage current, as well as better electrothermal stability.

Key-words: Varistor ceramics; Electroceramics; Electrothermal stability.

¹ Paper submitted for presentation at the 60th ABM Annual International Congress, July 2005, Belo Horizonte, Brazil.

² M.Sc. (Doctoral student), Researcher, Special Technologies Department, Electric Power Research Center, CEPEL, P.O.Box 68007, 21940-970, Rio de Janeiro, Brazil. e-mail: furtado@cepel.br

³ Senior Technician, Special Technologies Department, Electric Power Research Center, CEPEL, Rio de Janeiro, Brazil.

⁴ D.Sc., Research Consultant, R&D Directorate, Electric Power Research Center, CEPEL, Rio de Janeiro, Brazil

⁵ Engineer., Head, Special Technologies Department, Electric Power Research Center, CEPEL, Rio de Janeiro, Brazil

⁶ D.Sc., Professor, Department of Metallurgical and Materials Engineering, Federal University of Rio de Janeiro, P.O.Box 68505, 21945-970, Rio de Janeiro, Brazil.

INTRODUCTION

Zinc oxide (ZnO)-based semiconducting polycrystalline ceramics are scientific and technologically important materials because their grain and grain boundary properties which give origin to the varistor electrical characteristics of these materials. Although the non-linear (non-ohmic) current-voltage (I-U) characteristics of a varistor is still not completely understood, several works (CLARKE, 1999, p. 485; GUPTA, 1990, p. 1817; EDA, 1989, p. 28; SANTHANAM *et al.*, 1979, p. 852) connect the nonlinear behavior to the microstructure of the varistor material. These devices are used as voltage transient suppressor in a large variety of electric power systems and electro-electronic circuits (GUPTA, 1990, p. 1817; EDA, 1989, p. 28).

The I-U characteristics of a varistor are altered after some time under electrical bias. This behavior is known as degradation phenomena and manifests itself mainly by alterations in the pre-breakdown and onset of the breakdown regions of the I-U varistor curve (MANTAS *et al.*, 1986, p. 679; CASTRO *et al.*, 1993, p. 341). As a result, the varistors have a tendency of increasing in leakage current (I_L), in the pre-breakdown regime, with increasing time and temperature. Thus, the load life of ZnO varistors is restricted by the electrothermal runaway because of the increase of the leakage current under electric load. Therefore, the reduction of the leakage current is an important problem of the varistor technology (LAGRANGE, 1991, p. 1; CLARKE, 1999, p. 485) and can be reached by the adequate control of the microstructural parameters, such as grain boundary chemical composition, grain size distribution, densification level, and phase structure (NÓBREGA *et al.*, 1996, p. 1504; LAGRANGE, 1991, p. 1; GUPTA, 1987, p. 231).

ZnO varistors are divided generally into two categories, called Bi_2O_3 -based and Pr_6O_{11} -based varistors, in terms of varistor-forming oxides inducing the nonlinear properties of varistors (MUKAE, 1987, p. 1329). Most of the commercial ZnO varistors are Bi_2O_3 -based varistors, which have been mainly studied in various aspects since ZnO varistors were discovered by Matsuoka (1971, p. 736). However, Bi_2O_3 -based ZnO varistors are not suitable to be used in multilayer chip varistors manufacture, due to Bi_2O_3 having a high volatility and reactivity (MUKAE, 1987, p. 1329; TAKEHANA *et al.*, 1996, p. 186). Furthermore, in general, Bi_2O_3 -based ZnO varistors possess four phases, namely ZnO grains, Bi-rich intergranular layers, an additional insulating spinel phase, which does not play any role in electrical conduction, and pyrochlore phase. On the other hand, in Pr_6O_{11} -based ZnO varistors only two phases are present in a sintered body, namely, ZnO grains and the intergranular phase composed mainly of praseodymium oxide (CHUN, 1997, p. 995). The absence of a spinel phase increases the active grain boundary through which the electrical current flows. Therefore, the effective cross-section area of the element is increased. Earlier studies about Pr_6O_{11} -based varistors have been limited to the ternary system ZnO- Pr_6O_{11} -CoO and dissimilarities between Bi_2O_3 -based and Pr_6O_{11} -based ZnO varistors (MUKAE, 1987, p. 1329; ALLES *et al.*, 1993, p. 2098). Recently, many works have been made in order to study the influence of other rare-earth oxides (such as Y_2O_3 , Nd_2O_3 , Er_2O_3 , and Dy_2O_3) on the microstructural and electrical properties of the ternary system ZnO- Pr_6O_{11} -CoO, and the varistors produced have exhibited a relatively good electrical performance (NAHM *et al.*, 2000, p. 271; NAHM *et al.*, 2002, p. 110). In the present work it was evaluated the microstructural features and electrothermal behavior of two types of ZnO-based varistor ceramics (one, ZnO-

Pr₆O₁₁-based, and other ZnO-Bi₂O₃-based), obtained from different ceramic powder preparation methods (conventional ceramic route and chemical preparation process) and the results were applied to the understanding of the varistor performance. The analyzed systems, with chemical composition and powder preparation method, are shown in Table 1.

Table 1. Chemical composition and preparation method of the varistor ceramic investigated systems.

System	Chemical composition (mol%)
ZB ¹	96.5·ZnO-0.5·Bi ₂ O ₃ -1.0·Sb ₂ O ₃ -1.0·CoO-0.5·MnO-0.5·Cr ₂ O ₃
ZB-Q ²	96.5·ZnO-0.5·Bi ₂ O ₃ -1.0·Sb ₂ O ₃ -1.0·CoO-0.5·MnO-0.5·Cr ₂ O ₃
ZP ¹	97.59·ZnO-1.00·Pr ₆ O ₁₁ -1.00·Co ₃ O ₄ -0.20·B ₂ O ₃ -0.20·CaO-0.01·Al ₂ O ₃
ZP-Q ³	97.59·ZnO-1.00·Pr ₆ O ₁₁ -1.00·Co ₃ O ₄ -0.20·B ₂ O ₃ -0.20·CaO-0.01·Al ₂ O ₃

¹ Conventional ceramic method (solid state reactions).

² Chemical synthesis method: coprecipitation (FERREIRA, 1999, p. 82).

³ Chemical synthesis method: impregnation of salts (DUARTE, 2000, p. 90).

EXPERIMENTAL

Appropriate molar reagent grade powders were used to prepare the ZnO-based varistor ceramics. The sample compositions are shown in Table I. The ZB and ZP powders with adequate compositions were ball milled with zirconia balls in isopropyl alcohol media inside of a zirconia jar for 24 h. The ZB-Q and ZP-Q powders were obtained, respectively, in accord with the coprecipitation method (FERREIRA, 1999, p. 82) and salts impregnation technique (DUARTE, 2000, p. 90). The resultant mixtures were dried at 110⁰C for 12 h and calcined in air at 500⁰C (ZB and ZB-Q systems) and 750⁰C (ZP and ZP-Q systems) for 3 h. The calcined mixtures were granulated in a 200-mesh sieve and pressed into discs of 12.4 mm in diameter and 2.1 mm in thickness at a pressure of (80 ± 5) MPa. The discs were sintered at 1200, 1250, 1300, and 1350⁰C in air atmosphere for 2 h. The heating and cooling rates were 5⁰C/min. The average size of the final samples was 10.2 mm in diameter and 1.1 mm in thickness. The sintered bodies were sanded and polished, silver paste was coated on both faces of the samples and the silver electrode was formed by heating at 600⁰C for 10 min. The electrodes areas were approximately 0.22 cm².

The I-U characteristics of ceramics were measured using a curve tracer source-measurement unit (Tektronix 577). The breakdown electric field (E_B) was measured at 1.0 mA/cm² and the leakage current density (J_L) was measured at 80% of breakdown electric field. In addition, the nonlinear coefficient (α) was estimated for current-density range of 1.0 – 10.0 mA/cm². Additionally, the sample microstructures were examined by scanning electron microscopy (SEM, ZEISS DSM 960) applied on the polished (and 6M-NaOH aqueous solution-etched surface) and fractured surface of samples, and the microchemical compositional analysis was determined by an attached X-ray energy dispersive spectroscopy (EDS, Oxford ISIS) system. The crystalline phases were identified by powder X-ray diffraction (XRD, Diano XRD-8545, λCuKα radiation). The activation energies for the electrothermal behavior of the resistive component of the leakage current (I_{LR}), in the 25-175⁰C temperature range, were estimated from a plot of the resistive current versus temperature according to Arrhenius equation:

$$I_{LR}(T) = K_0 \cdot \exp\left(-\frac{E}{kT}\right) \quad (1),$$

where $I_{LR}(T)$ is the resistive current at temperature T (absolute temperature, in Kelvin), K_0 is a pre-exponential factor corresponding to I_{LR} at the initial temperature, E is the activation energy, and k is the Boltzmann constant. The I_{LR} evolution with respect to time (at constant temperature of 80°C) was estimated from the equation:

$$\Delta I_{LR} = I_{LR}(t) - I_{LR}(0) = K_R t^n \quad (2),$$

where ΔI_{LR} is the time-dependent increase in I_{LR} , K_R is an effective rate constant, $I_{LR}(0)$ is I_{LR} at time zero, and n a time exponent that gives a measure of the degree of stability of the device (for the most commercial varistors n is equal to 0.5). All the results that are presented in this paper constitute the average value for four samples of each type and condition, and the error bars (when necessary, in function of the scale in each case) indicate the discrepancy in relation to the average value.

RESULTS AND DISCUSSION

The Figure 1 shows the microstructural and electrical parameters evaluated for the varistor ceramic systems studied in function of the sintering temperature employed. It was verified that, for both chemical compositions considered, the average grain size (d_G) values of the systems obtained from ceramic powders chemically produced (Fig. 1(a)) are significantly smaller than those produced from conventional ceramic powders. In fact, chemical preparation methods, make possible the attainment of fine or ultrafine powders, although also increasing the probability of the aggregate formation (YAN, 1984, p. 106; FERREIRA, 1999, p. 82).

The Fig. 1(b) shows the densification degree of the studied systems. These results indicate that the biggest values of density were obtained by the sintering at 1200°C (for ZB and ZB-Q systems, corresponding to smallest average grain size achieved) and at 1300°C (for ZP and ZP-Q systems; but in this case it does not correspond to smallest d_G). For the ZB and ZB-Q systems the subsequent increase of the sintering temperature resulted in the increase of the porosity, probably due to Bi_2O_3 losses by volatilization (GUPTA, 1990, p. 1817). Additionally, and according to previous considerations, can be seen in Figure 2, the granulometric distribution of the powders obtained from chemical methods are narrower than those of the powders produced by conventional ceramic method, and besides, it was showed that the ZP and, mainly, ZP-Q systems present greater proportion of particle fractions below to $5 \mu\text{m}$, making possible to reach greater densification degree, such as shown in Figure 1(b).

The Figures 1(c) to 1(e) denote that optimized values of the fundamental varistor parameters (α , E_B , and J_L) were obtained in the respective sintering conditions that provide the greatest densification levels for both systems analyzed. In fact, as the densification degree decreases, thus occur the degeneration of the varistor properties, mainly it was verified a significative increase of the leakage current, as shown in Figure 1(e). This behavior is in accordance with the heat dissipation factor analysis (in alternate current) presents in Figure 1(f), which shows that the greatest values of D are associated with the ZB system, showing little reduction for ZB-Q

system. In addition, it was noted that, on the average, the D values for the ZP and ZP-Q systems are significantly lower than the present by ZB and ZB-Q systems, mainly in the low frequency region, in which varistors are typically used in overvoltage protection devices, denoting that the microstructure and chemical composition of the ZP and ZP-Q systems are more stable, of the viewpoint of the dielectric losses. In fact, varistor systems with the chemical composition of the type ZB/ZB-Q (conventional varistors) present polyphasic microstructures in which some phases do not play a part in the electrical conduction process that occurs in varistor ceramics (GUPTA, 1990, p. 1817; HE *et al.*, 2004, p. 138).

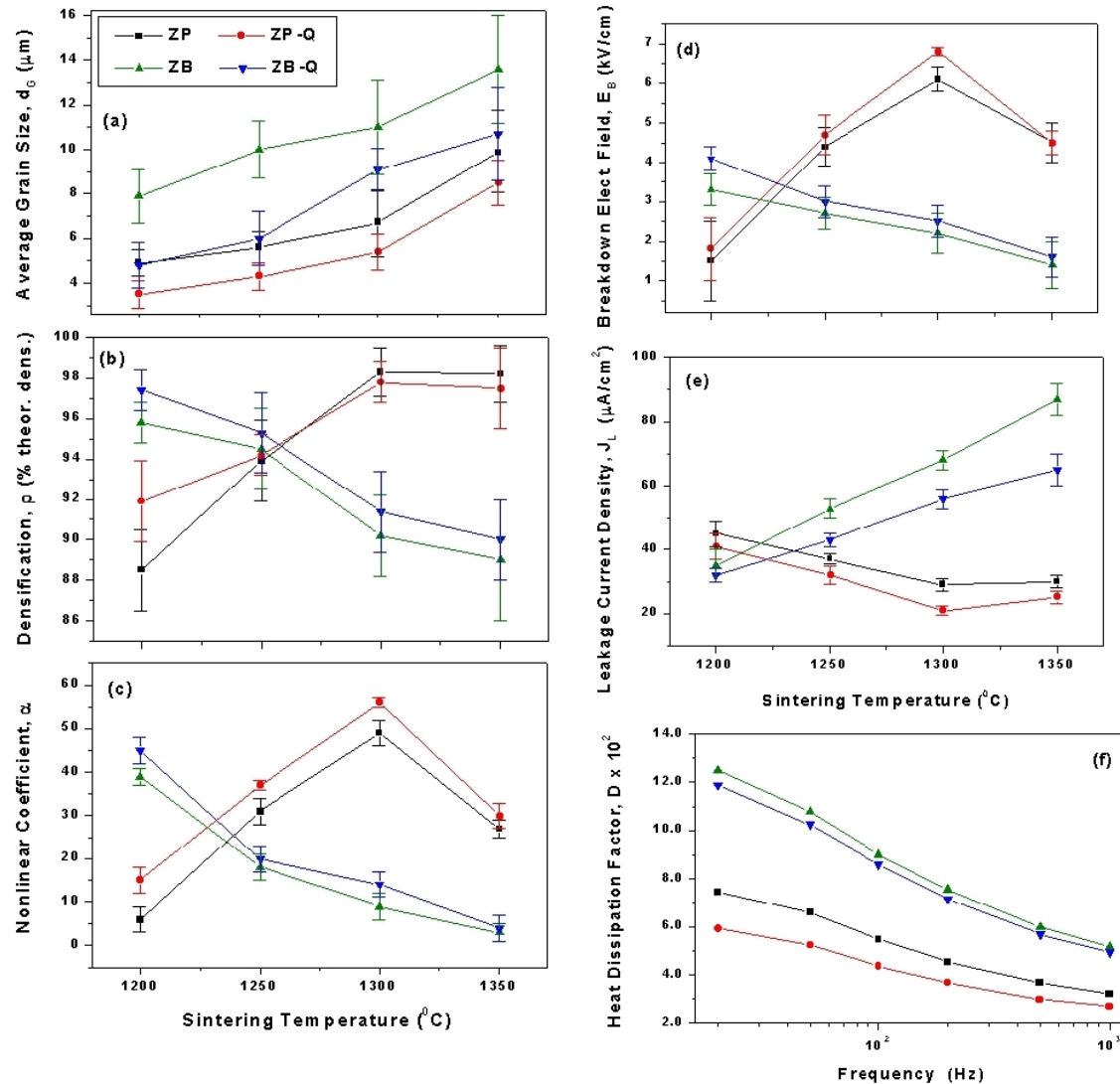


Figure 1. Microstructural and electrical parameters of investigated varistor ceramic systems in function of the sintering temperature: (a) Average grain size, (b) Densification degree (percentage of the theoretical density), (c) Nonlinear coefficient, (d) Breakdown electric field, (e) Leakage current density. (f) Heat dissipation factor analysis in function of the frequency of the applied alternate current (in this case, ZB and ZB-Q sintered at 1200^oC, and ZP and ZP-Q sintered at 1300^oC).

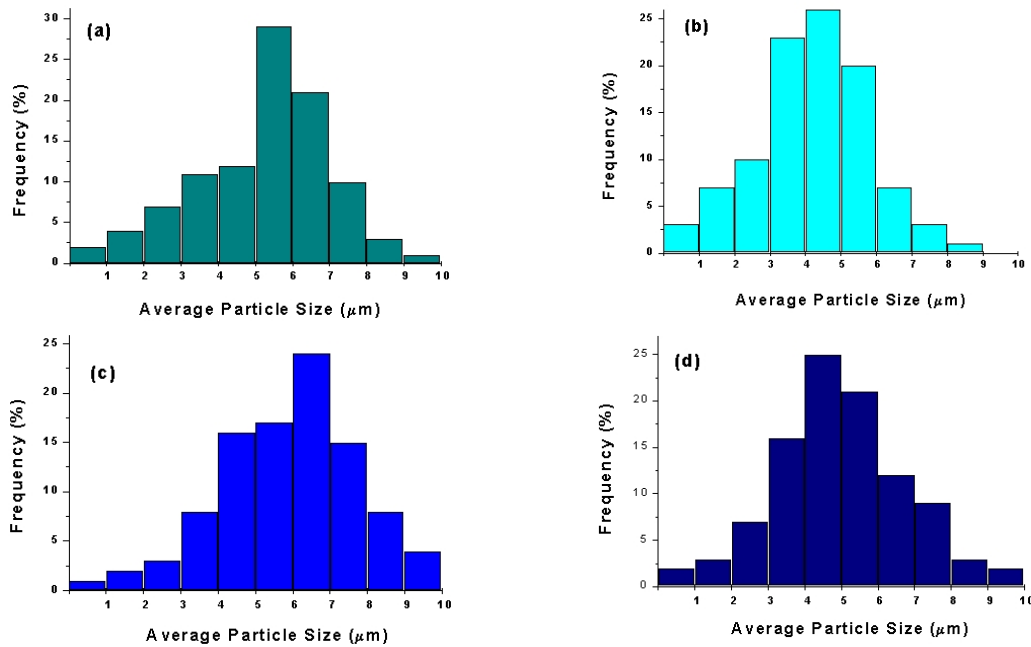


Figure 2. Particle size distribution (frequency histogram) of the ceramic powders used in the production of the varistor studied systems: (a) ZP, (b) ZP-Q, (c) ZB, (d) ZB-Q.

In conventional varistors, the complex microstructures and the phase transformations that take place along the sintering process can result in the porosity increase (GUPTA, 1990, p. 1817; MUKAE, 1987, p. 1329), such as evidenced in Figure 1(b), what will be reflected on the electrical characteristics, mainly on the leakage current, as shown in Figure 1(e). As a matter of fact, the electrothermal runaway of a varistor ceramic is associated with the resistive leakage current increase with respect to time, temperature, and bias cycle, which present greater probability of occurrence in devices characterized by microstructures with lower physical-chemical homogeneity, since that the presence of porosities, phases segregated at the grain boundary region (in high volumes) and phase variability, result in the formation of microstructural zones that present different temperature and current density profiles, in which the degradation process is originated (LAGRANGE, 1991, p. 1; HE *et al.*, 2004, p. 138). These considerations are in agreement with the results present in this work, since the ceramic samples that present lower densification degree, in general, exhibit the worse varistor characteristics. Besides, it was verified that the varistor properties of the ZP and ZP-Q systems are larger than those of the ZB and ZB-Q systems, as consequence of a greater microstructural homogeneity (MUKAE, 1987, p. 1329; LEE *et al.*, 1996, p. 2379). The Figure 3 shows the results of the SEM-EDS microstructural analysis of the evaluated systems, and the Figure 4 shows the XRD patterns of sintered ZB (evidencing its multiphase structure) and ZP (presents only ZnO and Pr-rich phases) varistor ceramic systems. The Figure 3(d) shows the ceramic powder characteristic of the ZP-Q system, which presents more regular forms and better dispersion condition in connection to its better varistor characteristics.

The electrothermal behaviors of the I_{LR} are illustrated in Figure 5(a) for the varistor ceramic systems studied. It was noted that there are two temperature ranges that I_{LR} presents distinct behaviors: a low temperature range (25-75°C) and a high

temperature range (100-175°C). The values of the activation energies and pre-exponential factor, for the varistor systems analyzed, were obtained from the linear regression fit of the Arrhenius plots shown in Figure 5(a), and these results are presented in Table 2. The Figure 5(b) shows the ΔI_{LR} time-dependent evolution curves and K_R (I_{LR} increment rate) obtained values for each system studied.

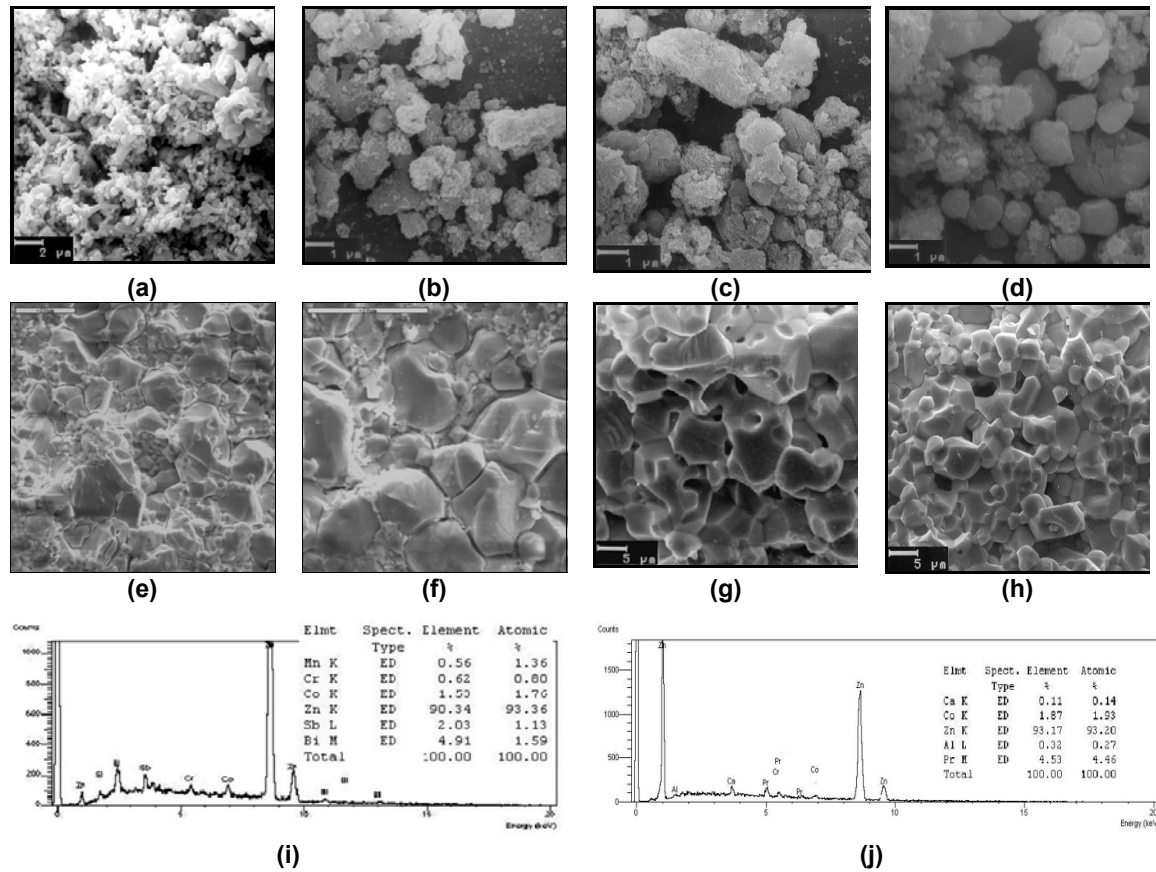


Figure 3. SEM-EDS microstructural analysis of the evaluated systems. Photomicrographs of powders: (a) ZB, (b) ZB-Q, (c) ZP, (d) ZP-Q. Photomicrographs of the fractured surface: sintered at 1200°C - (a) ZB, (b) ZB-Q; and sintered at 1300°C - (c) ZP, (d) ZP-Q. Typical chemical EDS analysis: (i) ZB, (j) ZP.

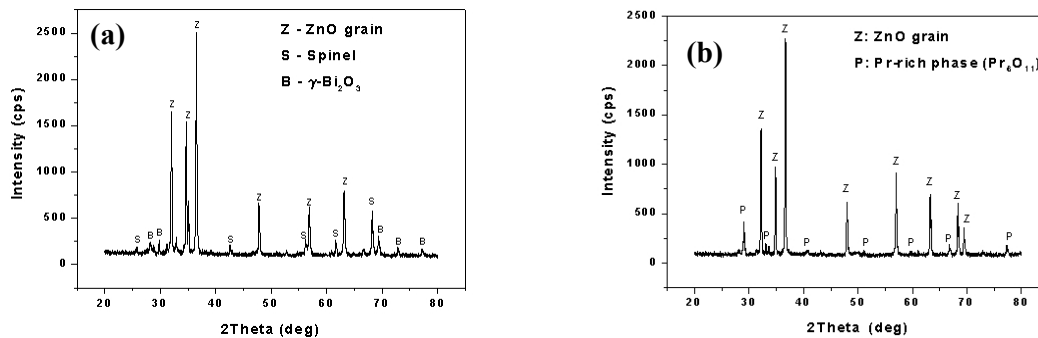


Figure 4. XRD patterns of (a) ZB sintered at 1200°C, and (b) ZP sintered at 1300°C varistor ceramic systems.

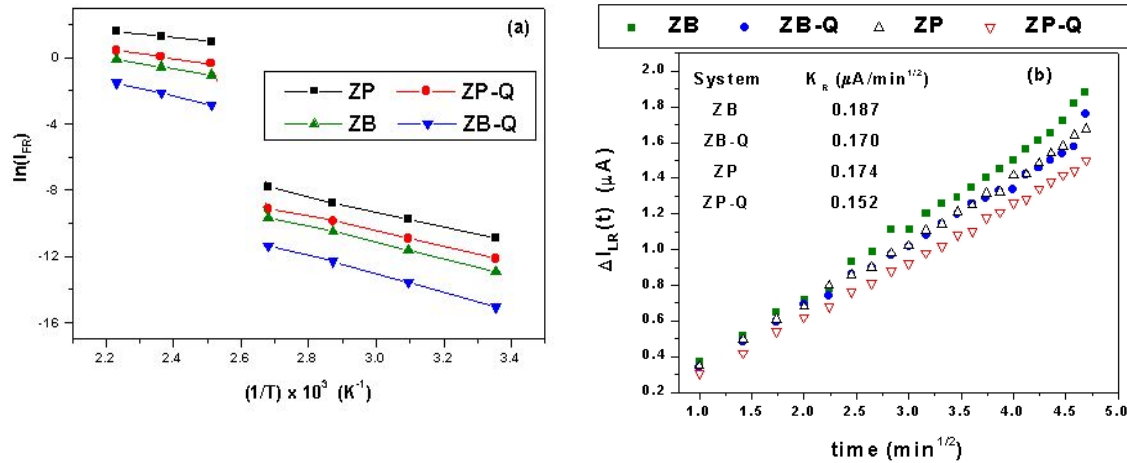


Figure 5. (a) Electrothermal behavior according to Arrhenius plots of I_{LR} , and (b) ΔI_{LR} curves (at constant temperature of 80°C), for the varistor ceramic systems studied.

Table 2. Activation energy (E , in eV) and pre-exponential factor (K_0 , in μA) for the varistor ceramic systems ZB, ZB-Q, ZP, and ZP-Q.

Temp. Range	25-75 $^{\circ}\text{C}$		100-175 $^{\circ}\text{C}$	
	Parameters ^{1,2}			
Systems ³	K_0	E	K_0	E
ZB	33	0.343	368	0.176
ZB-Q	35	0.349	385	0.183
ZP	31	0.370	381	0.210
ZP-Q	38	0.384	390	0.228

¹ Mean of the three samples of each type.

² Average discrepancy (δ) (all samples): $\delta E \cong 0.4\%$; $\delta K_0 \cong 0.9\%$.

³ ZB and ZB-Q sintered at 1200°C ; ZP and ZP-Q sintered at 1300°C .

The results of the Figure 5 and of the Table 2 indicate that the varistors produced from chemically prepared powders are more stable than those prepared by conventional ceramic process, since the first ones resulted in an increase (about 7 to 12%) in the respective activation energy values associated with the thermal evolution of I_{LR} , mainly at high temperature range. This observation is in accord with the ΔI_{LR} analysis, which shows that the ZP-Q system presented the slowest I_{LR} growth (smaller K_R values), since as much as bigger K_R value, then greater will be the trend to electrothermal degradation of the device, inasmuch as the ΔI_{LR} will grow more quickly.

CONCLUSIONS

It was verified that the zinc oxide-based varistor ceramics doped with rare-earth oxides showed better electrical characteristics than the conventional varistors, exhibiting particularly values of leakage current density near the half of the value of that characteristic of the conventional system. In general, varistors produced from chemically prepared powders exhibited better electrical and dielectric behaviors than those obtained by means of the traditional ceramic process. For a fixed chemical composition, a narrower particle size distribution of the precursor powder resulted in varistors with smaller values of leakage current density, as well as better

electrothermal stability, inferred from the analysis of the resistive leakage current behavior.

REFERENCES

1. CLARKE, D. R. Varistor Ceramics. **J. Am. Ceram. Soc.**, v.82, n.3, p. 485-502, 1999.
2. GUPTA, T. K. Application of Zinc Oxide Varistors. **J. Am. Ceram. Soc.**, v.73, n.7, p. 1817-1840, 1990.
3. EDA, K. Zinc Oxide Varistors, **IEEE Electrical Insulation Magazine**, v.5, n.6, p. 28-41, 1989.
4. SANTHANAM, A. T., GUPTA, T. K., CARLSON, W. G. Microstructural Evaluation of Multicomponent ZnO Ceramics, **J. Appl. Phys.**, v.50, n.2, p. 852-859, 1979.
5. MANTAS, P. Q., SENOS, A. M. R., BAPTISTA, J. L. Varistor-capacitor characteristics of ZnO ceramics, **Journal of Materials Science**, v.21, pp. 679-686, 1986.
6. CASTRO, M. S., BENAVENTE, M. A., ALDAO, C. M. Degradation in ZnO Varistors, **J. Phys.: Condens. Matter.**, v.5, p. A341-A342, 1993.
7. LAGRANGE, A. Present and Future of Zinc Oxide Varistors. In: **Electronic Ceramics**, edited by STEELE, B. C. H., Elsevier Applied Science, London, UK, p. 1-27, 1991.
8. NÓBREGA, M. C. S., MANNHEIMER, W. A. Varistor Performance of ZnO Based Ceramics Related to their Densification and Structural Development, **J. Am. Ceram. Soc.**, v.79, n.6, p. 1504-1508, 1996.
9. GUPTA, T. K. Effect of Material and Design Parameters on the Life and Operating Voltage of a ZnO Varistor, **J. Mater. Res.**, v.2, n.2, p. 231-238, 1987.
10. MUKAE, K. Zinc Oxide Varistors with Praseodymium Oxide, **Am. Ceram. Soc. Bull.**, v.66, n.9, p. 1329-1331, 1987.
11. MATSUOKA, M. Non-ohmic Properties of Zinc Oxide Ceramics, **Jpn. J. Appl. Phys.**, v.10, n.6, p. 736-746, 1971.
12. TAKEHANA, M., NISHINI, T., SUGAWARA, K., SUGAWARA, T. Preparation of Zinc Oxide Varistors by a Wet Chemical Method, **Materials Sci. Engineering Bull.**, v.41, p.186-189, 1996.
13. CHUN, S-Y., WAKIYA, N., FUNAKUBO, H., SHINOZAKI, K., MIZUTANI, N. Phase Diagram and Microstructure in the ZnO-Pr₂O₃ System, **J. Am. Ceram. Soc.**, v.80, n.4, p. 995-998, 1997.
14. ALLES, A. B., PUSKAS, R., CALLAHAN, G., BURDICK, V. L. Compositional Effects on the Liquid-Phase Sintering of Praseodymium Oxide-Based Zinc Oxide Varistors, **J. Am. Ceram. Soc.**, v.76, n.8, p. 2098-2102, 1993.
15. NAHM, C-W., PARK, C-H., YOON, H-S., Microstructures and varistor properties of ZnO-Pr₆O₁₁-CoO-Nd₂O₃-based ceramics. **J. Mater. Sci. Lett.**, v.19, p. 271-274, 2000.
16. NAHM, C-W., RYU, J-S., Influence of sintering temperature on varistor characteristics of ZPCCE-based ceramics. **Mater. Lett.**, v.53, p. 110-116, 2002.
17. FERREIRA, F. S. Controle na Química de Preparação, Dispersão e Mistura de Ingredientes na Consolidação de Microestruturas de Varistores de ZnO, Tese de M.Sc., COPPE/UFRJ, Rio de Janeiro, RJ, Brasil, 1999.
18. DUARTE, M. V. S. Síntese e Caracterização Elétrica e Microestrutural de Varistores à Base de ZnO Dopados com Óxidos de Terras-Raras, Tese de M.Sc., COPPE/UFRJ, Rio de Janeiro, RJ, Brasil, 2000.
19. YAN, M. F. Densification and Microstructural Development during Ceramic Processing. **Microstructure and Properties of Ceramic Materials**, Yen, T. S., Pask, J. A. (ed.), p.106-124, 1984.
20. HE, J., ZENG, R., CHEN, Q., CHEN, S., GUAN, Z., HAN, S-W., CHO, H-G. Nonuniformity of Electrical Characteristics in Microstructures of ZnO Surge Varistors. **IEEE Transactions on Power Delivery**, v. 19, n. 1, p. 138-144, 2004.

COMPORTAMENTO ELETROTÉRMICO E CARACTERÍSTICAS MICROESTRUTURAIS DE CERÂMICAS VARISTORAS À BASE DE ÓXIDO DE ZINCO ¹

José Geraldo de Melo Furtado ²
Luiz Antônio Saléh ³
Eduardo Torres Serra ⁴
Jorge Henrique Greco Lima ⁵
Maria Cecília de Souza Nóbrega ⁶

Resumo

Os aspectos concernentes à corrente de fuga existente em varistores à base de óxido de zinco sob diversas condições de operação são de fundamental importância para o projeto e especificação desses dispositivos utilizados em sistemas de proteção contra sobretensões. Este trabalho tem por objetivo investigar as relações entre características microestruturais e a estabilidade eletrotérmica de cerâmicas varistoras à base de óxido de zinco. Os resultados evidenciam que a corrente de fuga e a capacidade de um varistor de absorver e de dissipar energia dependem de vários parâmetros, tais como o grau de densificação do corpo cerâmico, a distribuição de fases precipitadas, a distribuição de tamanhos de grão e a homogeneidade composicional, além da composição química específica do dispositivo, especialmente os tipos de dopantes empregados. Varistores à base de ZnO dopados com terras-raras, exibindo microestrutura menos complexa que a dos varistores convencionais, apresentaram melhor comportamento dielétrico. Para uma composição química fixa, uma estreita distribuição de tamanho de partícula proporcionou menores valores de corrente de fuga, bem como melhor estabilidade eletrotérmica.

Palavras-chave: Varistores; Eletrocerâmicas; Estabilidade eletrotérmica.

¹ Trabalho submetido para apresentação no 60^o Congresso Anual da ABM, julho de 2005, Belo Horizonte, Brasil.

² M. Sc., Pesquisador, Depart. de Tecnologias Especiais, Centro de Pesquisa de Energia Elétrica, CEPEL/ELETOBRAS, Caixa Postal 68007, 21940-970, Rio de Janeiro, Brasil. e-mail: furtado@cepel.br

³ Técnico Sênior, Depart. de Tecnologias Especiais, Centro de Pesquisa de Energia Elétrica, CEPEL, Rio de Janeiro, Brasil.

⁴ D.Sc., Pesquisador-consultor, Diretoria de P&D, Centro de Pesquisa de Energia Elétrica, CEPEL, Rio de Janeiro, Brasil.

⁵ Engenheiro., Pesquisador-coordenador, Depart. de Tecnologias Especiais, Centro de Pesquisa de Energia Elétrica, CEPEL, Rio de Janeiro, Brasil.

⁶ D.Sc., Professor, Programa de Engenharia Metalúrgica e de Materiais, COPPE, Universidade Federal do Rio de Janeiro, C. P. 68505, 21945-970, Rio de Janeiro, Brasil.